Control Systems Analysis and Design

Article II

Jessé de Oliveira Santana Alves

November, 2021

Contents

1 Sampled Control System

1.1 Motivation

Control systems basically consist of a plant, a feedback sensor and a controller (Figure 1). The blueprint of a system, that is, the object to be controlled is, in most cases, analog devices, therefore, they are mathematically modeled as continuous systems over time. However, due to reliability, flexibility and precision, digital transconductors are used as sensors and digital embedded systems are used as controllers in most cases. When comparing, for example, an analog device with a digital device, it is clear that analog devices, when designed, often require resistors, capacitors and inductors with non-commercial values, making them difficult and expensive to obtain, and consequently leading to approximations in terms of design that reduces the accuracy of the devices. Furthermore, computers when used as digital controllers can be configured and reconfigured for various applications and conditions, storing data and performing complex calculations. Unlike analogues that do not have this flexibility when changing components. Finally, it is seen that, over time, microcontrollers and digital devices have become cheaper and more accessible.

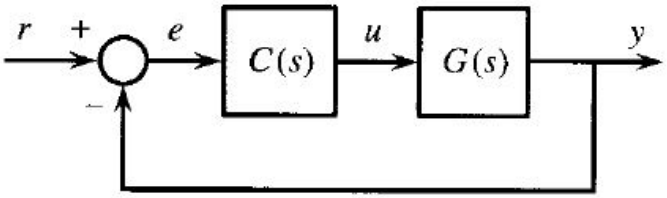

Figure 1: Basic components of a control system.

In this sense, control systems with the presented characteristics can be described in general by the block diagram of **??**. Where $R(z)$ and $E(z)$ are the Z-transforms of the reference signal and error signal respectively. And $Y(s)$, $Q_u(z)$ and $Q_y(z)$ are the Laplace transforms of the output signals, input perturbation and output perturbation, respectively. Furthermore, $F(z)$ represents the digital reference filter, $C(z)$ the digital controller, $G(s)$ the analog plant of the system to be controlled and SoZ represents the zero order insurer which converts the digital signal leaving $C(z)$ into an analog signal $U(s)$.

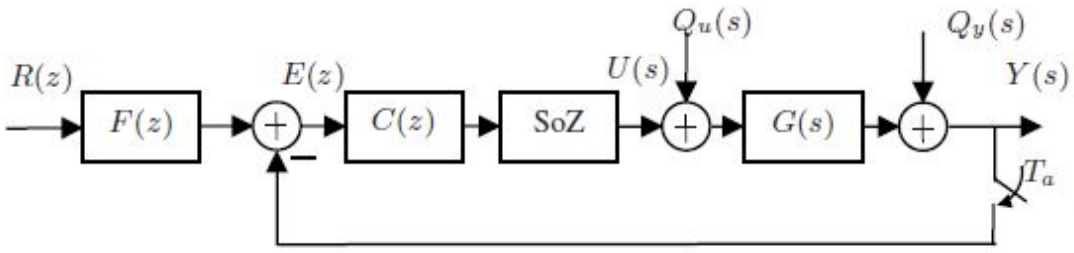

Figure 2: Control System Sampled with Reference Filter

Therefore, as most control systems are fundamentally described by the **??** block diagram, developing techniques for implementing sampled controllers is essential knowledge for a control systems designer. Along this path, the methodologies for the discrete-time project addressed in this Challenge IV will be: the allocation of poles, without canceling the zeros and poles of the model, and the controller based on the internal model (IMC). In the pole allocation procedure, prior determination of the location of each root of the characteristic closed-loop polynomial allows the designer to have greater control over the system's behavior, guaranteeing stability and performance, since the modes of a system determine its behavior over time. The IMC controller, in addition to following the allocation strategy, allows you to cancel poles and zeros from the process, thus ensuring better reference tracking and disturbance rejection.

1.2 Simulations performed

For this challenge, given the sampled control system from **??**, the plant $G(s)$ is described by the transfer function

$$G(s) = \frac{0,2(10-s)}{(s+1)^2}, \tag{1}$$

and the controller and reference filter are given by:

$$C(z) = \frac{S(z)}{R(z)}, \tag{2}$$

$$F(z) = \frac{T(z)}{S(z)}, \tag{3}$$

where $S(s)$, $R(s)$ and $T(s)$ are polynomials to be determined in the pole allocation process and, subsequently, in the IMC control.

The first step of this project was to determine the desired settling time value of 2% for the system. To do this, the output signal vectors y and the time t were first obtained using the function *step()*. Subsequently, using the $find()$ function, the time was found in which the vector y reached 98% of the steady state, thus determining the settling time of $G(s)$ in the open loop:

$$t_{s_{MA}} = 5.82\ s$$

.

Thus, as a performance criterion, the settling time t_s must be approximately half of this value, therefore, it was defined:

$$t_s = 3\ s.$$

Then, the sampling period T_a was determined based on the following empirical rule

$$T_a = \frac{t_{s_{5\%}}}{20}, \tag{4}$$

where T_a is the settling time of 5%. Therefore, in this work, following the same previous methodology, modifying only the value of 95% of the final value, we obtained:

$$T_a = 0.24. \tag{5}$$

Having determined these parameters, in the pole allocation project, the strategy used to meet a t_s of 3 seconds was to allocate two repeated poles, based on the equation

$$t_{s_{2\%}} = 6\tau, \tag{6}$$

where τ is the time constant. Therefore, for $t_s = 3\ s$, $\tau = 0.5$, and consequently, the closed-loop poles are

$$s_1 = s_2 = -2.$$

However, as the project also requires step-type reference following and the rejection of constant disturbances, both at the output and input, as criteria, the controller must have an integrating term $(z-1)$. Therefore, in order to reconcile these requirements, together with the criterion that the degree of the controller's denominator must be greater than or equal to that of the plant's denominator, in this project, the controller will have two poles, and consequently, the closed-loop system will have four poles. Thus, so that the allocation of these last two poles does not interfere with the accommodation time criterion, the principle of modal dominance is used, allocating them 15 times further away than s_1 and s_2. Soon,

$$s_3 = s_4 = -30.$$

Having defined the closed-loop poles of the system, the following algorithm was implemented in *MATLAB*:

The poles were converted to discrete time using the equation $z = e^{T_a s}$, obtaining:

$$z_1 = 0.6129; \quad z_2 = 0.6129; \quad z_3 = 0.0007; \quad z_4 = 0.0007.$$

Then, the coefficients of the characteristic polynomial (D_0) that has these roots were determined, using the function *poly()*, finding

$$D_0 = 0 - 0.0005z + 0.3773z^2 - 1.2270z^3 + z^4; \tag{7}$$

The system plan (1) was discretized using the zero order insurer with the sampling period 5, resulting in

$$G(z) = \frac{0.0119z + 0.0804}{z^2 - 1.571z + 0.6166}; \tag{8}$$

So, for the poles z_1, z_2, z_3 and z_4 to be allocated, the coefficients of the controller transfer function (Equation 9) were determined through the system of equations **??**, resulting from the development of the Diophantina equation.

$$C(z) = \frac{B_2z^2 + B_1z + B_0}{A_2z^2 + A_1z + A_0}, \tag{9}$$

$$\begin{bmatrix} A_0 \\ B_0 \\ A_1 \\ B_1 \\ A_2 \\ B_2 \end{bmatrix} = M^{-1} \begin{bmatrix} P_0^T \\ \mathbf{0} \end{bmatrix}, \tag{10}$$

where P_0^T is the transposed vector of the coefficients of the desired characteristic polynomial (7), and the matrix M is given by

$$\begin{bmatrix} 0.6166 & 0.0809 & 0 & 0 & 0 & 0 \\ -1.5705 & 0.0119 & 0.6166 & 0.0804 & 0 & 0 \\ 1 & 0 & -1.5705 & 0.0119 & 0.6166 & 0.0804 \\ 0 & 0 & 1 & 0 & -1.5705 & 0.0119 \\ 0 & 0 & 0 & 0 & 1 & 0 \\ \mathbf{-1} & \mathbf{0} & \mathbf{-1} & \mathbf{0} & \mathbf{-1} & \mathbf{0} \end{bmatrix}, \tag{11}$$

where the matrix coefficients are given by an arrangement of the plant coefficients 8. And the terms in bold were placed with the aim of meeting the relation 12, which forces an integrator in the controller's transfer function. The development of this process is given by

$$\begin{gathered} A_2z^2 + A_1z + A_0 = (z-1)(a_1z + a_2), \\ A_2z^2 + A_1z + A_0 = a_1z^2 + (a_2 - a_1)z - a_2, \\ A_0 = -a_2; \quad A_1 = a_2 - a_1; \quad A_2 = a_1, \\ A_1 = -A_0 - A_2, \\ -A_0 - A_1 - A_2 = 0. \end{gathered} \tag{12}$$

Solving **??**, we obtain the following transfer function for the controller

$$C(z) = \frac{17.4510(z^2 - 1.4070z + 0.4997)}{(z + 1.1360)(z - 1)} \tag{13}$$

Finally, the reference filter was defined so that its denominator $S(z)$ is equal to the controller numerator, and the filter numerator $T(z)$ in order to cancel the additional poles of closed loop z_3 and z_4. And then, after normalizing the DC gain of $F(z)$, resulting in

$$F(z) = \frac{0.0931(z - 0.0007)}{(z^2 - 1.4070z + 0.4997)} \tag{14}$$

Once $C(z)$ and $F(z)$ were determined, the **??** system was temporally simulated using a *script* with extension .m in *MATLAB* , with $R(z) = \frac{z}{z-1}$, $Q_u(s) = 0.2\frac{e^{-40s}}{s}$ and $Q_y(s) = 0.2\frac{e^{-20s}}{s}$.

In the second stage of the challenge, the controller design based on the internal model began by defining the discrete-time plant as:

$$P_n(z) = \frac{B^+(z)B^-(z)}{A(z)}, \tag{15}$$

where $A(z)$ is the denominator of $P_n(z)$, $B^+(z)$ represent the minimum phase zeros and $B^-(z)$ represent poorly damped zeros, or non-minimum phase, which cannot be canceled in this process. To achieve this, the first step was to use the discretized system plan **??**, here called $P_n(z)$, given in factored form as

$$P_n(z) = \frac{0.0119(z + 6.7790)}{(z - 0.7853)^2}; \tag{16}$$

then, comparing the equations **??** and **??**, we obtain that

$$B^-(z) = (z + 6.7790). \tag{17}$$

Subsequently, two central transfer functions of the IMC methodology are defined: $H_d(z)$, which represents the behavior between the reference input and the system output, and the robustness filter $F_r(z)$, which represents the complementary sensitivity function of the process, given by

$$F_r(z) = B^-(z)\tilde{F}_r(z), \tag{18}$$

$$H_d(z) = B^-(z)\tilde{H}_d(z), \tag{19}$$

where $\tilde{F}_r(z)$ and $\tilde{H}_d(z)$ are functions arbitrated in order to guarantee the project performance criteria. For reasons of causality, the relative degree of $F_r(z)$ must be greater than or equal to that of $P_n(z)$ and the relative degree of $H_d(z)$ greater than or equal to that of $F_r(z)$. Finally, the reference filter and controller of the IMC project are defined as

$$C_{BMI}(z) = \frac{F_r(z)P_n^{-1}(z)}{1 - F_r(z)}, \tag{20}$$

$$F(z) = \frac{H_d(z)}{F_r(z)}. \tag{21}$$

In this way, $\tilde{F}_r(z)$ is arbitrated as

$$\tilde{F}_r(z) = \frac{0,16}{(z - 0,6)^2}, \tag{22}$$

in order to offer a settling time of 2% in closed loop equal to 3 seconds, as previously specified, and so that $F_r(z)$ has a relative degree equal to $P_n(z)$. Therefore, multiplying 17 and 22, we obtain

$$F_r(z) = \frac{0.16(z + 6.7790)}{(z - 0.6)^2}. \tag{23}$$

Then, as $F_r(z)$ represents the complementary sensitivity function of the process, 23 is normalized so that the DC gain is unity, thus guaranteeing the system reference tracking. Soon,

$$Gain_{DC} = F_r(1) = 7.779, \tag{24}$$

therefore, normalized $F_r(z)$ is given by

$$F_r(z) = \frac{0.0206(z + 6.7790)}{(z - 0.6)^2}. \tag{25}$$

Then, using the transfer functions **??** and 25 in the equation **??**, we obtain the IMC controller of this project, given by

$$C_{BMI}(z) = \frac{1.7348(z - 0.7853)^2}{(z - 1)(z - 0.22)}. \tag{26}$$

Finally, with the aim of using a strategy that has only one degree of freedom, we set $F_r(z) = H_d(z)$, arbitrating only the $\tilde{F}_r(z)$. Consequently, making the reference filter (Equation 18) unitary. Then, similarly to the case of pole allocation, the **??** system is simulated with the same conditions and the same values of the reference signal and input and output disturbances.

1.3 Results obtained

As a result of the developments described, given the controller (Equation 2) and the reference filter (Equation 3), the following were obtained for the controller project by pole allocation polynomials

$$S(z^{-1}) = 17.45 - 24.55z^{-1} + 8.72z^{-2},$$

$$R(z^{-1}) = 1.00 + 0.14z^{-1} - 1.14z^{-2},$$

$$T(z^{-1}) = 1.6250 - 0.0023z^{-1} + 0z^{-2}.$$

In the temporal simulation, given the disturbance signals from Figure 3,

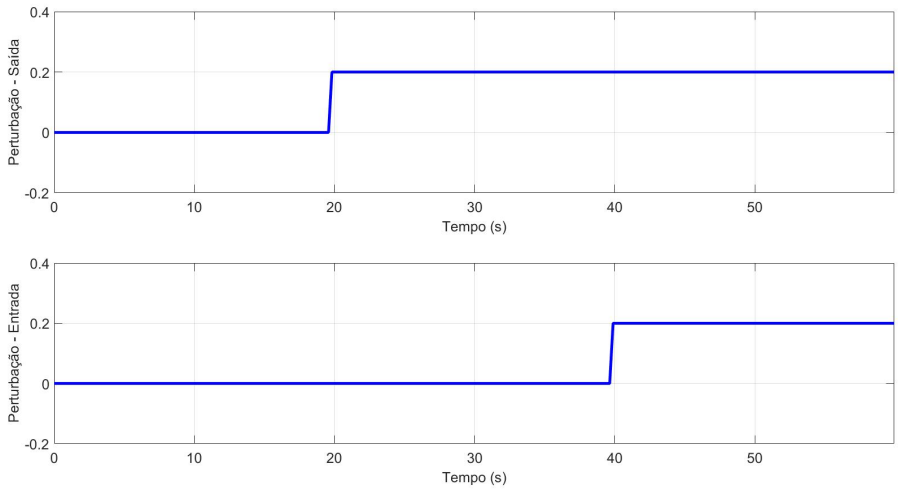

Figure 3: Entry and exit disturbance signals.

the following graphs were obtained for the output signal and control signal of the system,

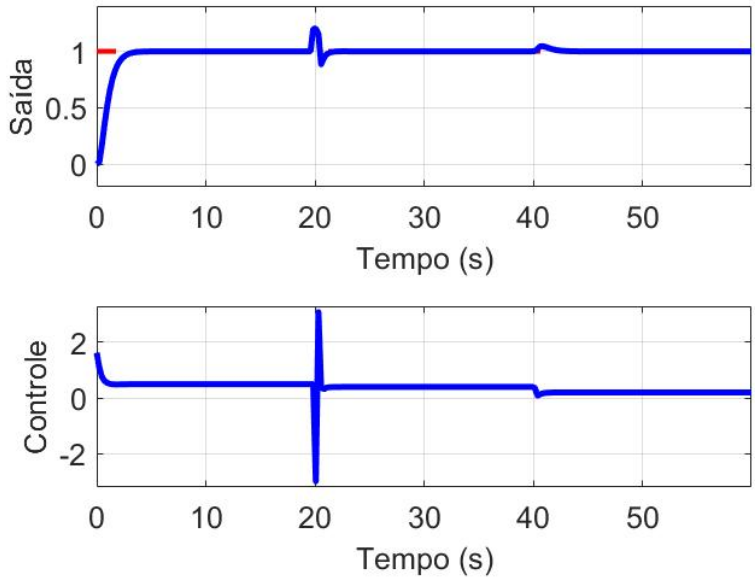

Figure 4: Output signal and simulation control signal with pole allocation control.

guaranteeing the predicted accommodation time of 2%, with

$$t_{s_{2\%}} = 3.1426\ s$$

In the IMC controller project, given the same configurations and conditions as the first project, the following result was obtained

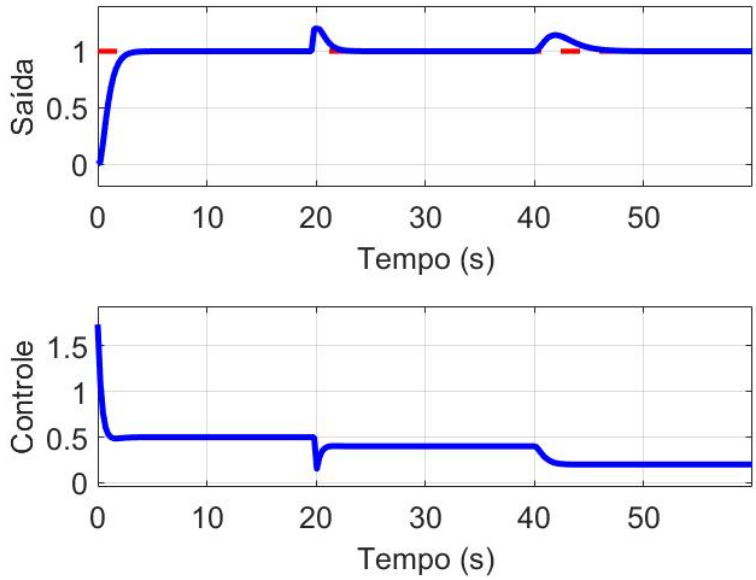

Figure 5: Output signal and control signal of the simulation with IMC control.

with accommodation time:

$$t_{s_{2\%}} = 2.9009\ s$$

When analyzing the simulations in figures 4 and 5, it is observed that both reference tracking and disturbance rejection were successfully met in both projects. However, in the process of rejecting pole allocation disturbances, the control signal presents sudden and higher oscillations in the output disturbance when compared to the IMC control, probably due to the non-minimum phase zero in the controller. On the other hand, in pole allocation, the controller is able to more effectively reject the input disturbance when compared to the IMC controller. However, despite these differences, according to theory, it is possible to obtain a better result in rejecting input disturbances with the IMC controller. All that is needed is for perturbation rejection to be accelerated by designing a modified IMC. This process is carried out by placing a stable pole inside $B^{-}(z)$, in order to avoid its cancellation. Furthermore, it is worth mentioning that, for the model's zeros to be canceled, the controller must have poles in the right half plane (SPD) of *s*, since these zeros are of non-minimum phase. This, in turn, would directly affect the internal stability of the system, as any modeling uncertainty or variations in plant parameters would make this unstable pole manifest in the system's output signal.

1.4 Conclusions

It can be seen that in both cases the criteria of accommodation time of approximately 3 seconds, reference follow-up and rejection of constant disturbances were met. To do this, it was necessary to force one pole of the controller onto the unit circle of the z plane, in order to integrate the constant error signal, and consequently, follow the reference. Furthermore, in both cases a normalization process was necessary in some system transfer functions, in order to make the DC gain unity. In the case of pole allocation, this process occurred in the reference filter $F(z)$, and in the IMC controller in the robustness filter $F_r(z)$. In general, both the pole allocation design methodology and the internal model design methodology proved to be efficient in developing the sampled controller. Since in both cases the performance criteria were satisfied for the system $G(s)$. It should be noted, however, that the IMC controller had a lower cost for the control signal necessary for this achievement.

2 Multivariable Control in State Space

2.1 Motivation

A system that has multiple inputs and multiple outputs, from the English *multiples-inputs/multiples-outputs* (MIMO), is also defined as a multivariable system. These systems - often complex - require controllers capable of dealing with these diverse inputs and outputs, ensuring stability and performance. To achieve this, the design of these systems is usually carried out in state space, that is, both the system representation and the controller design are carried out with this mathematical representation. This is because the state equations of a system provide a highly general mathematical representation, including the use of matrices that facilitate the analysis, synthesis and optimization of systems. This matrix representation is given by:

$$\dot{x}(t) = Ax(t) + Bu(t), \tag{27}$$
$$y(t) = Cx(t) + Du(t), \tag{28}$$

where $x(t) \in \mathbb{R}^n$ is the state vector, $y(t) \in \mathbb{R}^q$ is the output signal vector, $u(t) \in \mathbb{R}^m$ is the control signal vector, $A \in \mathbb{R}^{n \times n}$, $B \in == zzmathbbR^{n \times m}$, $C \in \mathbb{R}^{q \times n}$ and $D \in \mathbb{R}^{q \times m}$.

Regarding the controller, while in classical control projects, the strategy for meeting performance criteria is based on closed-loop modal dominance, in the project represented in state space, control is done by state feedback (== zzautoreffig:real$_e stado_d iagrama$), $where the designer has the possibility of specifying all closed-loop poles of the system, t$

$$u(t) = -Kx(t), \tag{29}$$

where $K \in \mathbb{R}^{m \times n}$ is called the state feedback gain matrix.

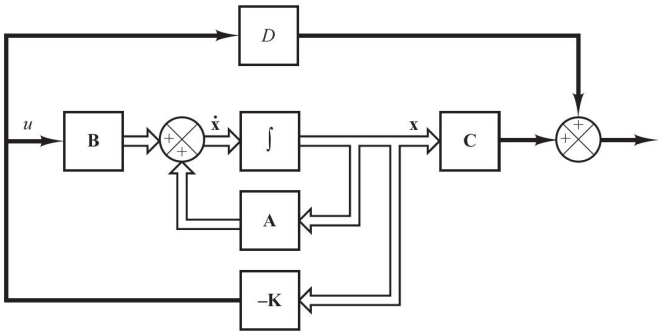

Figure 6: Block diagram of a control system with state feedback.
Source: Adapted from (OGATA,2014).

In this control strategy, it is still possible to insert an integral action into the system, in order to guarantee reference tracking with a certain robustness. In this case, the error signal is integrated and multiplied to a gain K_i, as shown in Figure 7. Furthermore, the state feedback gain matrix K can be obtained by several mathematical strategies, either by allocating the closed-loop poles or by solving an optimization problem (LQR being the most popular), in which a matrix Optimal K is determined by weighing the system performance with the control effort.

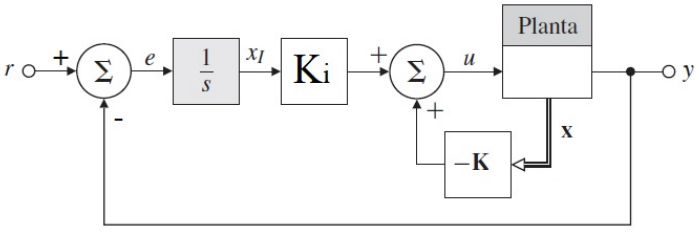

Figure 7: Control system with state feedback with integrator.
Source: Adapted from (FRANKLIN; POWELL; EMAMI-NAEINI, 2013).

2.2 Simulations performed

In this challenge, we want to design a state feedback controller, whose output is taken to the following condition:

$$\lim_{t\to\infty} y(t) = y_{eq} = [2\ 1]^T.$$

To achieve this, the first step was to determine the system sampling time, following the criteria that:

$$\frac{t_s}{20} < T_a < \frac{t_s}{10} \tag{30}$$

where T_a is the sampling period and t_s is the settling time of 2%. Therefore, given the sampled system of **??** with $G(s)$ given by

$$G(s) = \begin{bmatrix} \frac{2}{(10s+1)} & \frac{0,8}{(10s+1)(2s+1)} \\ \frac{0,6}{(10s+1)(2s+1)} & \frac{1,5}{(10s+1)} \end{bmatrix}, \tag{31}$$

the settling time of 2% was calculated for each transfer function within the $G(s)$ matrix.

Subsequently, using Equation 30, the lowest possible value was obtained for the sampling period such that it satisfied all transfer functions of $G(s)$. Once this was done, an equilibrium control vector was calculated such that $u_{eq} = G(0)^{-1} y_{eq}$.

Then, $G(s)$ was represented - with minimal realization - in the state space, using the function *ss()* for the conversion. Then, given these matrices in continuous time, using the equation

$$x_{eq} = -A^{-1} B u_{eq},$$

the equilibrium state vector x_{eq} was calculated.

After these steps, the system $G(s)$ was discretized and represented in the state space, then, using the equation

$$x_{eq} = (I - A_d)^{-1} B_d u_{eq},$$

determine the equilibrium state vector through the matrices in discrete time. And as the last step of this process, the value of y_{eq} was validated, calculating the following equation:

$$y_{eq} = C_d x_{eq},$$

with C_d and x_{eq} determined by the process described above.

So, as a next step, two projects were carried out: one to determine the state feedback gain for the system with a configuration similar to **??**, and another for the system with a configuration similar to Figure 7. For the first, closed-loop discrete-time poles approximately equal to:

$$\lambda_j = e^{-\frac{T_a}{4}}.$$

Thus, using the *place()* function from *MATLAB*, the matrix A_d and B_d was passed together with a vector with all poles in λ_j. Later, in the second project, with the insertion of the integral action in the system, the matrices

A, B and C are resized due to the addition of the state vector with the integral of the error. Thus, the augmented system is defined as:

$$\begin{bmatrix} \Delta x[k] \\ y[k+1] \end{bmatrix} = \begin{bmatrix} A & 0 \\ FALLS & \end{bmatrix} \begin{bmatrix} \Delta x[k] \\ y[k] \end{bmatrix} + \begin{bmatrix} B \\ CB \end{bmatrix} \Delta u[k] \tag{32}$$

Thus, using the same procedure as in the first project, the six closed-loop eigenvalues were allocated to λ_j. Once this was done, the two control systems were simulated, one with state feedback without an integrator and the other with an integrator. Subsequently, a state observer was inserted for both cases and the system was simulated again.

2.3 Results obtained

As a result of this challenge, the accommodation times of each system were first obtained separately:

$$\begin{aligned} t_{a_{11}} = t_{a_{22}} &= 39.1439\ s, \\ t_{a_{12}} = t_{a_{21}} &= 40.3413\ s. \end{aligned} \tag{33}$$

Then, using the criterion 30, we arrived at the following value for the sampling period:

$$T_a = 2.07\ s,$$

subsequently, calculating the equilibrium control vector, we obtained:

$$u_{eq} = \begin{bmatrix} 0.8730 \\ 0.3175 \end{bmatrix}. \tag{34}$$

When taking the system $G(s)$ to the state space, the following matrices were determined:

$$A = \begin{bmatrix} -0.1668 & -0.0842 & -0.1683 & 0.0842 \\ -0.0441 & -0.5055 & -0.0111 & -0.0945 \\ -0.0881 & 0.0639 & -0.3721 & 0.1861 \\ 0.0441 & 0.0555 & 0.1111 & -0.1555 \end{bmatrix}, \quad B = \begin{bmatrix} 0.3181 & 0.0000 \\ -0.1877 & 0.5000 \\ -0.3754 & -0.0000 \\ 0.1877 & 0.5000 \end{bmatrix},$$

$$C = \begin{bmatrix} 0.3320 & -0.1905 & -0.0610 & 0.1905 \\ 0.1926 & 0.1044 & 0.2088 & 0.1956 \end{bmatrix}, \quad D = \begin{bmatrix} 0 & 0 \\ 0 & 0 \end{bmatrix},$$

to then determine the equilibrium state vector, given by:

$$x_{eq} = \begin{bmatrix} 4.0606 \\ -0.7913 \\ -0.7889 \\ 2.3786 \end{bmatrix}. \tag{35}$$

In discrete time, the calculated state space matrices are:

$$A_d = \begin{bmatrix} 0.7366 & -0.0963 & -0.1926 & 0.0963 \\ -0.0504 & 0.3489 & -0.0127 & -0.1081 \\ -0.1009 & 0.0732 & 0.5016 & 0.2130 \\ 0.0504 & 0.0636 & 0.1271 & 0.7495 \end{bmatrix}, \quad B_d = \begin{bmatrix} 0.7014 & 0.0000 \\ -0.2805 & 0.5722 \\ -0.5611 & 0.1813 \\ 0.2805 & 0.9349 \end{bmatrix},$$

$$C_d = \begin{bmatrix} 0.3320 & -0.1905 & -0.0610 & 0.1905 \\ 0.1926 & 0.1044 & 0.2088 & 0.1956 \end{bmatrix}, \quad D_d = \begin{bmatrix} 0 & 0 \\ 0 & 0 \end{bmatrix},$$

then, calculating x_{eq} in discrete time, we obtained:

$$x_{eq} = \begin{bmatrix} 4.0606 \\ -0.7913 \\ -0.7889 \\ 2.3786 \end{bmatrix}, \tag{36}$$

which is, exactly, the equilibrium state vector calculated in continuous time 35. And, finally, by calculating the value of y_{eq}, the expected value was also obtained:

$$y_{eq} = \begin{bmatrix} 2 \\ 1 \end{bmatrix}.$$

In the controller design, all closed-loop poles were allocated to:

$$\lambda_j = e^{-\frac{T_a}{4}} = 0.5960,$$

therefore, applying the function *place()* with four poles in λ_j, the feedback gain was obtained:

$$K_d = \begin{bmatrix} 1.8051e-01 & 8.9347e-02 & 1.7862e-01 & -8.9339e-02 \\ -1.7887e-06 & -1.1909e-01 & 7.5961e-02 & 3.2808e-02 \end{bmatrix}. \tag{37}$$

With the insertion of the integrator, the increased matrices A and B are given by:

$$A_d = \begin{bmatrix} 0.7366 & -0.0963 & -0.1926 & 0.0963 & 0 & 0 \\ -0.0504 & 0.3489 & -0.0127 & -0.1081 & 0 & 0 \\ -0.1009 & 0.0732 & 0.5016 & 0.2130 & 0 & 0 \\ 0.0504 & 0.0636 & 0.1271 & 0.7495 & 0 & 0 \\ 0.2699 & -0.0908 & -0.0679 & 0.1824 & 1.0000 & 0 \\ 0.1254 & 0.0456 & 0.0912 & 0.1983 & 0 & 1.0000 \end{bmatrix}, \quad B_d = \begin{bmatrix} 0.7014 & 0 \\ -0.2805 & 0.5722 \\ -0.5611 & 0.1813 \\ 0.2805 & 0.9349 \\ 0.3740 & 0.0580 \\ 0.0435 & 0.2805 \end{bmatrix}.$$

Therefore, applying *place()*, we obtained:

$$K_a = \begin{bmatrix} 0.296737 & -0.050091 & -0.042814 & 0.070822 & 0.325568 - 0.173654 & \\ 0.063262 & 0.021622 & 0.137543 & 0.244735 & -0.130194 & 0.434032 \end{bmatrix}, \tag{38}$$

$$K_i = \begin{bmatrix} 0.3256 & -0.1737 \\ -0.1302 & 0.4340 \end{bmatrix}, \tag{39}$$

where K_d is the state feedback gain and K_i the integrator gain. For the system without an integrator and without an observer, we obtained:

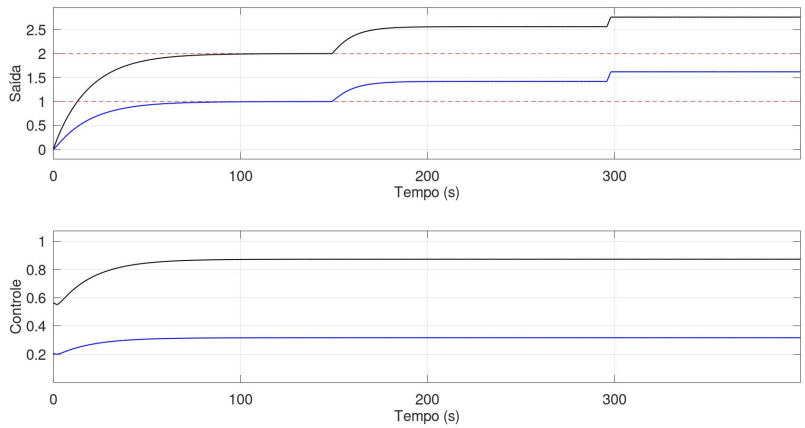

Figure 8: Temporal Simulation of the System without Integrator and without Observer.

For the system without an integrator and with an observer, we obtained:

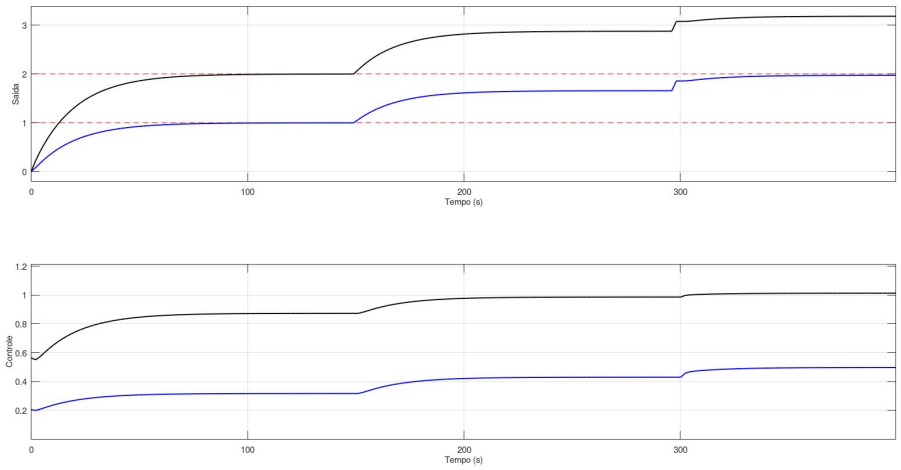

Figure 9: Temporal Simulation of the System without integrator and with observer.

For the system with integrator and without observer, we obtained:

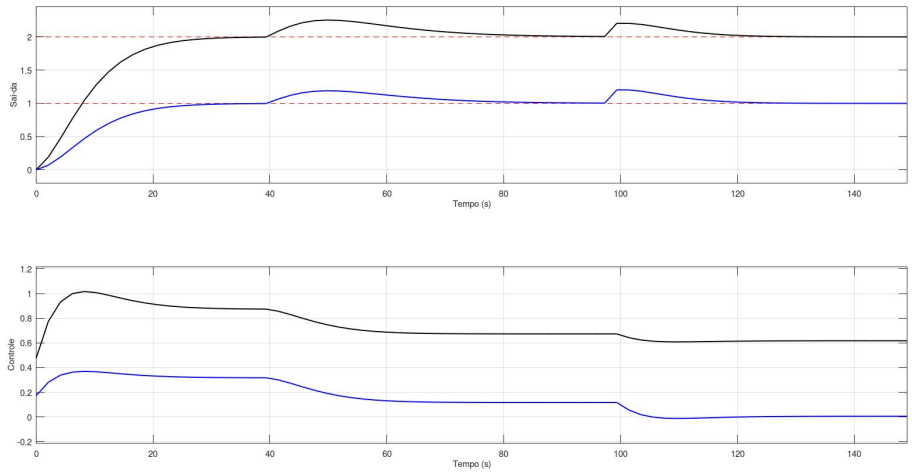

Figure 10: Temporal Simulation of the System with integrator and without observer.

For the system with integrator and observer, we obtained:

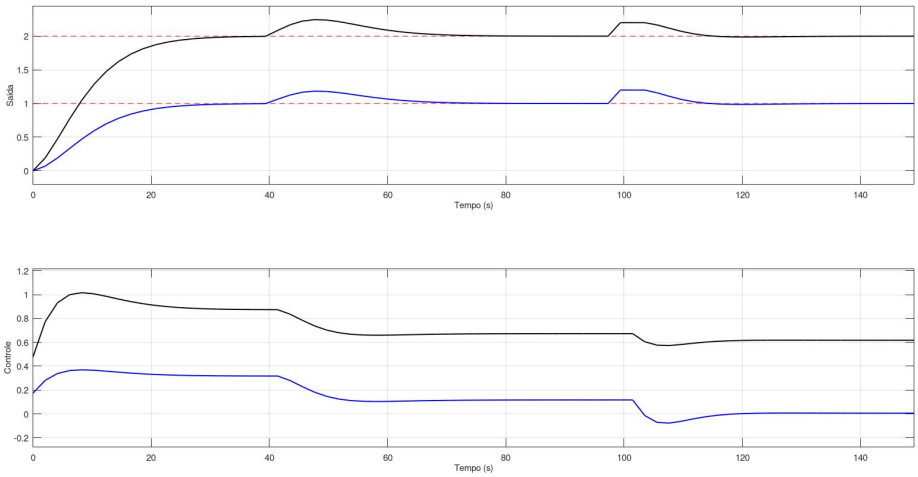

Figure 11: Temporal Simulation of the System with integrator and observer.

What was expected in theory is that both designed controllers would be capable of following the reference. However, in relation to rejecting disturbances, it is expected that the system with integral action follows the reference more robustly, therefore, rejects input and output disturbances, unlike the system without an integrator.

2.4 Conclusions

The state space representation of a system allows it to be described internally. This mathematical strategy describes the system in state equations that are effective in complex applications, such as nonlinear, time-varying and multivariable systems (MIMO). In this project, it was possible to verify the effectiveness of this approach for the $G(s)$ system with multiple inputs and multiple outputs, in which the allocation of poles via state feedback allows freedom to choose the system modes in strategic positions of the plane s, in order to guarantee stability and performance, such as, for example, desired settling time and overshoot. Furthermore, the inclusion of comprehensive action in this strategy guarantees robust reference monitoring for the system. This is excellent in cases where there are uncertainties in the model parameters and advantageous when compared to just adding a gain *feedforward* to the system reference signal. Finally, another effective point seen in this challenge is its application in systems where the states are not possible to be measured. In these cases, the creation of a state observer can meet the need for measurement, thus ensuring the possibility of designing with state feedback.

3 Non-Linear System Control

3.1 Motivation

Control systems often need to be developed to stabilize and bring performance to non-linear systems, such as *drones*, aircraft, and in this case, the Van der Pol oscillator. Control design For these types of systems, whose superposition principle is not valid, they can be carried out using different strategies, including linearization around an equilibrium point. The oscillatory system considered here has a convergence behavior for a limit cycle of defined amplitude, whatever the initial condition determined, except the origin. Therefore, in this challenge, the control technique chosen for this system will be LQR control, in which the quadratic linear regulator problem will be solved, minimizing the cost function J_∞, given by:

$$J_\infty = \int_0^\infty \Big[x^T(t)Qx(t) + u^T(t)Ru(t)\Big]dt, \tag{40}$$

where $x(t)$ is the state vector, $u(t)$ is the control signal vector, $Q \succeq 0$ ($Q \in \mathbb{R}^{n==zztimesn}$) and $R \succ 0$ ($R \in \mathbb{R}^{m\times m}$) are, respectively, the weighting matrices of the system state vector and control signal vector. And the terms $\big(x^T(t)Qx(t)\big)$ and $\big(u^T(t)Ru(t)\big)$ represent the distance from the state to the origin and the cost of the control signal, respectively.

Furthermore, the phase diagram of the Van der Pol oscillator - used to represent a vector field that estimates the trajectory followed by the system's states - will be developed, with the aim of evaluating stability in the vicinity of the desired equilibrium.

3.2 Simulations performed

In the present project, given the Van der Pol oscillator described by the following state equations in compact form,

$$\begin{bmatrix}\dot{x_1}(t)\\ \dot{x_2}(t)\end{bmatrix} = \begin{bmatrix}x_2(t)\\ -x_1(t) + 0.3(1 - x_1(t)^2)x_2(t) + u(t)\end{bmatrix}, \tag{41}$$

the first step consisted of finding two linearized models, one with the equilibrium point at $\overline{x}_1 = 1$ and $\overline{x}_2 = 0$, and the other at $\overline{x}_1 = 4$ and $\overline{x}_2 = 0$. Thus, taking the model to the following description:

$$\delta\dot{x}(t) = A\delta x(t) + B\delta u(t), \tag{42}$$

on what

$$A = \left.\frac{\partial f(x(t),u(t),t)}{\partial x}\right|_{x=\overline{x}\ \ u=\overline{u}}, \quad B = \left.\frac{\partial f(x(t),u(t),t)}{\partial u}\right|_{x=\overline{x}\ \ u=\overline{u}}, \tag{43}$$

where $\delta x(t) = x(t) - \overline{x}$ and $\delta u(t) = u(t) - \overline{u}$. Therefore, applying Equation 43 to the system 41, the following matrices were obtained, through the partial derivatives of the model 41:

$$A = \begin{bmatrix}0 & 1\\ -1 - 0.6x_1(t)x_2(t) & -0.3{x_1}^2 + 0.3\end{bmatrix}_{\substack{x=\overline{x}\\ u=\overline{u}}}, \quad B = \begin{bmatrix}0\\ 1\end{bmatrix}_{\substack{x=\overline{x}\\ u=\overline{u}}}, \tag{44}$$

and, subsequently, two linear models were determined replacing the equilibrium points. To then compare the eigenvalues of the matrix A of these two calculated models.

So, solving the quadratic linear regulator problem described in Equation 40, with $R = 0.1$ and $Q = I$, through the *lqr()* function of *MATLAB*, the state feedback gain K was obtained for the two calculated linear models. In sequence, using *Pplane*, executed by Java, the oscillator phase plane was obtained with the following control laws: (i) $u(t) = 0$, (ii) $u(t) = -K(x(t) - \overline{x}(t)) + \overline{u}$ with the LQR gain and the equilibrium values referring to the first model and (iii) $u(t) = 0$, (ii) $u(t) = -K(x(t) - \overline{x}(t)) + \overline{u}$ with the LQR gain and the relative equilibrium values to the second model. Finally, with the aim of validating the control laws mentioned above, they were all simulated using an integration step $dT = 0.01$ with the Euler method and initial condition $x(0) = [-5\ -5]^T$.

3.3 Results obtained

For this challenge, the first results obtained were the two linearized models. In the first model, for $\overline{x}_1 = 1$ and $\overline{x}_2 = 0$, the matrices were obtained:

$$A_1 = \begin{bmatrix} 0 & 1 \\ -1 & 0 \end{bmatrix}, \quad B_1 = \begin{bmatrix} 0 \\ 1 \end{bmatrix}, \tag{45}$$

and in the second model, for $\overline{x}_1 = 4$ and $\overline{x}_2 = 0$, we obtained:

$$A_2 = \begin{bmatrix} 0 & 1 \\ -1 & -4.5 \end{bmatrix}, \quad B_2 = \begin{bmatrix} 0 \\ 1 \end{bmatrix}. \tag{46}$$

Then, calculating the eigenvalues of A_1 and A_2, we have that:

$$\lambda_{1_{MODEL\ 1}} = j \quad e \quad \lambda_{2_{MODEL\ 1}} = -j,$$

It is

$$\lambda_{1_{MODEL\ 2}} = -0.2344 \quad e \quad \lambda_{2_{MODEL\ 2}} = -4.2656.$$

In order to evaluate the behavior of the system in both equilibrium positions, comparing these eigenvalues, it is concluded that, for the first model, the eigenvalues are on the imaginary axis of the plane s, that is, the system is marginally stable in around this balance point. In the second model, the eigenvalues are on the real axis, with a negative part, therefore, the system is stable around the second equilibrium point.

Subsequently, using the function *lqr()* for both models, the following state feedback gains were obtained:

$$K_1 = [2.3166 \quad 3.8253],$$

$$K_2 = [2.3166 \quad 1.4062].$$

Then, in the simulation part, both the phase diagram and the temporal simulation, via Euler, were applied to the three cases (i), (ii) and (iii).

In the first case, setting $u(t) = 0$, the following phase diagram was obtained:

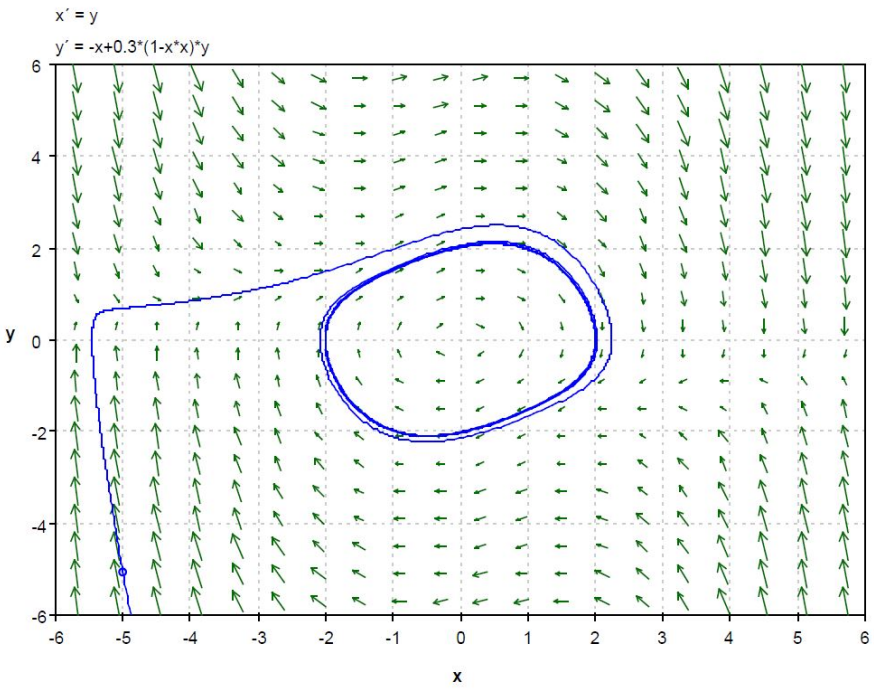

Figure 12: Phase diagram of the Van der Pol Oscillator with the control law of the first case.

And then the following temporal simulation:

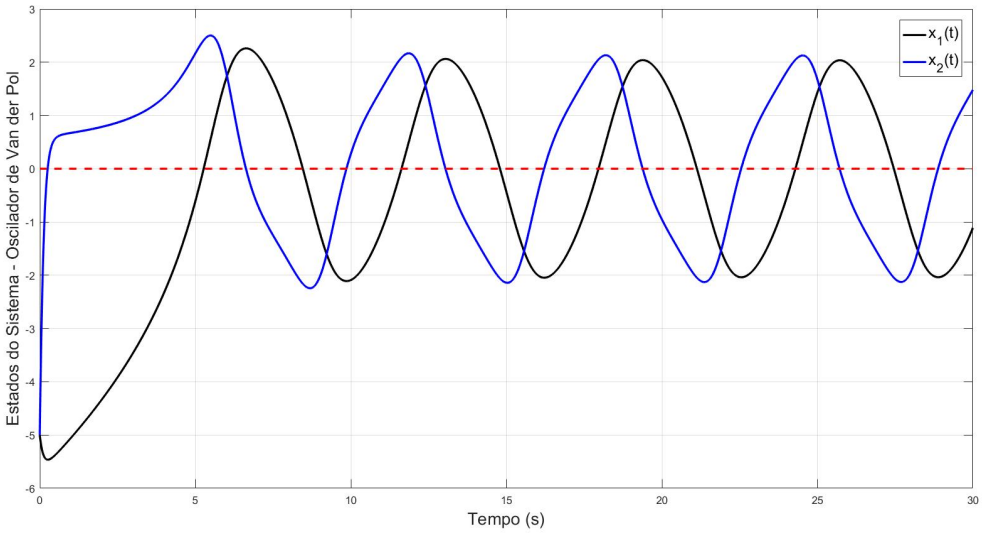

Figure 13: Temporal Simulation with the control law of the first case.

When analyzing Figure 12, an oscillatory behavior around the origin is observed. It is concluded, therefore, that the system does not reach the equilibrium point when the control signal $u(t)$ is equal to zero, instead, it oscillates around x_1 and x_2 equal to zero. This is also evaluated in the temporal simulation of Figure 13, in which both states, starting from the initial value of -5, do not diverge, but rather evolve towards an oscillatory behavior around zero, characterizing marginal stability. This was expected theoretically, since the Van der Pol oscillator manifests itself as a limit cycle.

For the second case, with the state feedback gain K_1 and equilibrium points at $\overline{x}_1 = 1$ and $\overline{x}_2 = 0$, we obtained the following results:

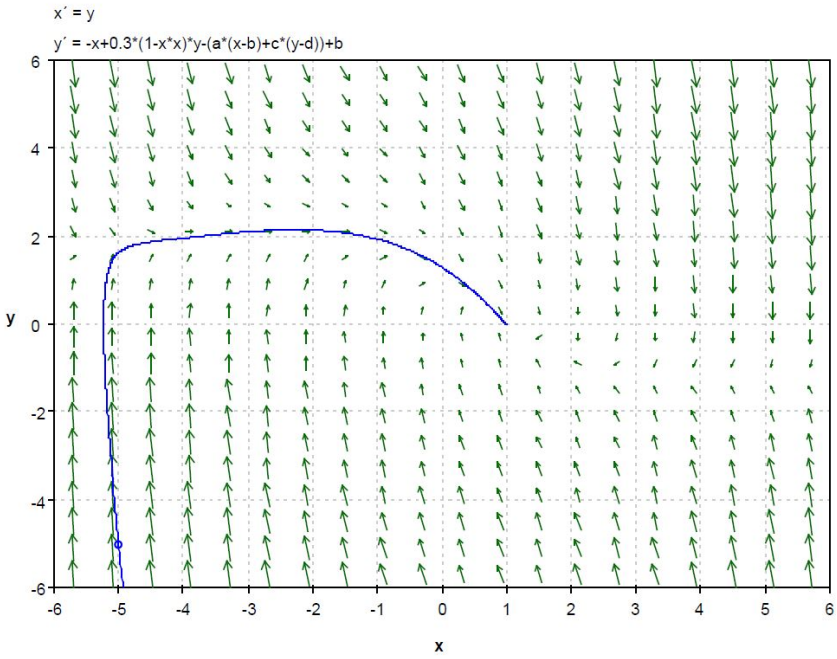

Figure 14: Phase diagram of the Van der Pol Oscillator with the control law of the second case.

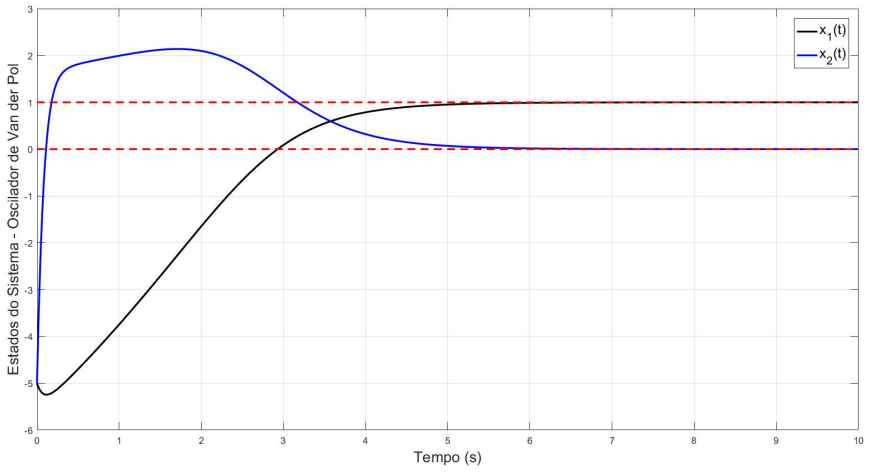

Figure 15: Temporal Simulation with the control law of the second case.

In this case, the control signal $u(t)$ is given by state feedback, with the feedback gain K calculated via LQR. Therefore, it can be seen in the Figure 14 diagram that the states converge to the equilibrium point $\overline{x}_1$ and $\overline{x}_2$. Observing from the trajectory in blue, that, in the initial moments of the simulation, starting from $x(0) = [-5 - 5]^T$, the state x_2 - represented by the vertical axis - moves much more faster than the state x_1, where the vector fields are practically vertical. This conclusion is consistent with the analysis of the temporal simulation shown in Figure 15, in which, in addition to the convergence of the states at the equilibrium points at practically the same time, the speed at the initial moments of the state x_2 is greater than the state x_1, generating an overshoot, and then returning to the equilibrium point. This situation can be seen in both simulations.

Finally, in the third and final case, with the state feedback gain K_2 and equilibrium points at $\overline{x}_1 = 4$ and $\overline{x}_2 = 0$, the following results were obtained:

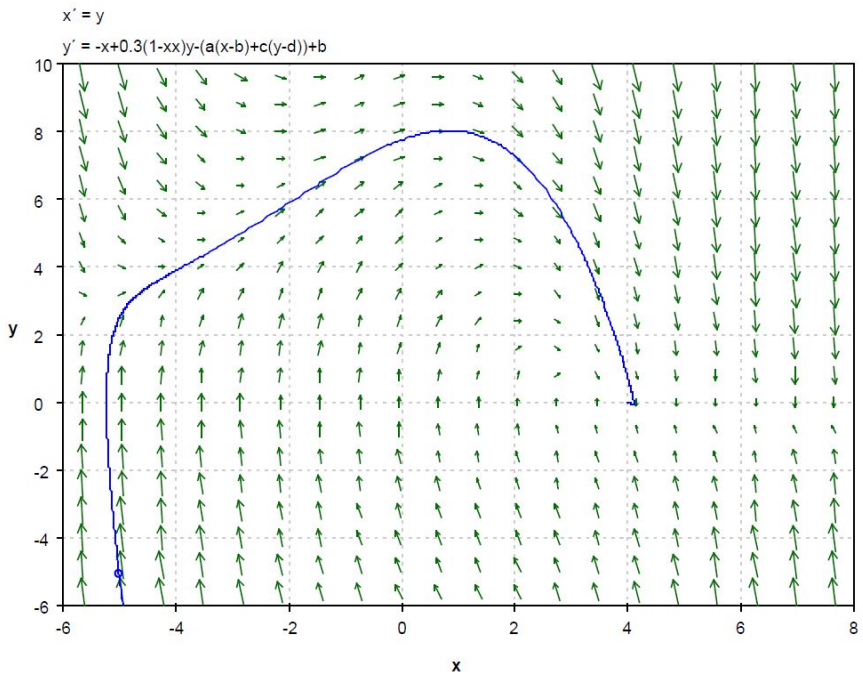

Figure 16: Phase diagram of the Van der Pol Oscillator with the control law of the third case.

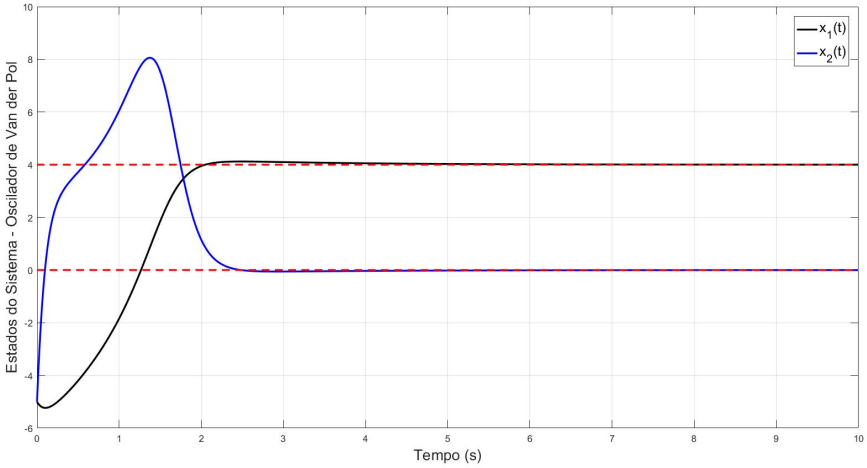

Figure 17: Temporal Simulation with the third case control law.

In the latter case, the system also converged to the equilibrium point, as can be seen in the Figure 16 diagram. Again, the state x_2 evolves more quickly, as in the second case, however, presenting a much larger overshoot this time, reaching the value 8 and then returning abruptly to the equilibrium point $\overline{x}_2 = 0$. The state x_1, on the other hand, follows a similar behavior to the second case, evolving practically without overshoot for the reference. This same analysis can be carried out by observing Figure 17. Furthermore, it is worth highlighting that the latter case, despite presenting a greater overshoot in the x_2 state, settles more quickly to the equilibrium point: the x_1 in approximately 2 seconds and the x_2 in approximately 2.5 seconds. While in the second case, this time is close to 5.5 seconds.

3.4 Conclusions

In this challenge, it was possible to analyze a control system, that is, its behavior, performance and stability, through the observation of simulations of the system's states, both temporally and through the phase diagram of *Pplane* . Following this strategy, an LQR controller was designed for a non-linear system, based on two linearized models at different equilibrium points. Given this, it was validated, firstly, that the system has an oscillatory behavior, around the origin, when starting from any point, except the origin. Later, it was noticed that, with the application of the control signal, the system converges to the specified equilibrium points, even in the first linearization model, in which the system presented marginal stability. Finally, it is noteworthy that in this Van der Pol oscillator, the state x_2 evolves faster than the state x_1 at the beginning of the system.